JOURNAL OF AIRCRAFT
Vol. 47, No. 2, March–April 2010

Multilevel Structural Optimization for Preliminary Wing-Box Weight Estimation

G. Bindolino,* G. Ghiringhelli,† S. Ricci,‡ and M. Terraneo§
Politecnico di Milano, 20156 Milan, Italy

DOI: 10.2514/1.41552

This paper deals with the weight estimation of the wing box of a commercial aircraft by means of a procedure suitable for very large liners and/or unconventional configurations for which statistical data and empirical formulas may not be sufficiently reliable. Attention is focused on the need to account for aeroelastic interaction from a very preliminary stage of the design cycle. The procedure exploits the first of three levels of a multilevel structural optimization system conceived for the preliminary design of the wing primary structure and a simplified evaluation of the cross-sectional properties. The comparison between weight estimates obtained with the present procedure and predictions supplied by available literature shows a satisfactory agreement.

Nomenclature

A_s	=	stiffener area
b	=	stiffener pitch
c	=	airfoil chord
D_2	=	summed squared distance of every stiffener from neutral axis
E	=	Young's modulus
h	=	airfoil averaged thickness
I_1, I_2, J	=	principal moment of inertia and torsional stiffness coefficient
k_c	=	coefficient related to critical stress of panels, depending on b/t ratio
N	=	number of stiffeners
t_e	=	equivalent thickness related to the stiffener
t_s	=	skin thickness
t_w	=	web thickness
η	=	roll effectiveness
σ_{Scr}, σ_{Pcr}	=	critical stresses for stiffeners and panels
τ_s	=	skin panel shear stress
τ_w	=	web panel shear stress
ν	=	Poisson's modulus
Ω	=	enclosed wing-box area

I. Introduction

THE conceptual design of commercial aircraft, especially in the case of very large civil transporters, will require effective weight prediction capabilities: the challenge of designing a liner with more than 600 seats, a takeoff maximum weight exceeding 500 t, and a wingspan of up to 80 m and more can no longer be supported by estimations based on empirical or statistical assumptions [1,2]. These considerations also apply to unconventional aircraft, for example, strut-braced wings, joined wings, and the PrandtlPlane® configuration, described in [3], that need very sophisticated design tools [4,5] and for which meaningful statistical data are not available. The aircraft global optimization needs a reliable estimate of the wing weight and should account for any kind of interaction with the wing structural design, for example, the center of gravity position. The wing weight is strongly dominated by the primary structure (i.e., the wing box); it affects the aircraft conceptual design, as well as its mass distribution, but static, dynamic, and aeroelastic behaviors of the wing can also pose a significant drawback to flight qualities and cruise strategies. In [6] it has been demonstrated how the simultaneous optimization of the wing planform, airfoil shape, and structural sizing can significantly improve the aircraft performance: here, the interaction is envisaged within the framework of a computational fluid dynamics (CFD) approach and a simplified analytical model to estimate the minimal material in term of skin weight. Despite the complexity of the approach, it may not be sufficient. In [7], the need for a correct introduction of requirements for torsional stiffness and aeroelastic behavior from conceptual design has been recognized. Indeed, a more general approach is also needed due to other remarks, for example, the availability of a number of affordable technologies (e.g., active control of flutter, active control for gust alleviation, etc.) suitable for the design of lighter wings should be carefully accounted for from very preliminary design steps to gather the maximum advantage and weight saving.

Multidisciplinary design optimization seems to be a very promising approach [8,9], allowing the integration of different design disciplines such as flight mechanics, performances, aerodynamics, structures, systems, and costs; but difficulties arise when many disciplines have to be used simultaneously, exhibiting poor couplings in both object function and constraints sensitivities [10,11]. Concurrent [12] and cooperative [13] engineering represents a modus operandi that can better support a design to account for interaction between different partners. Multilevel decomposition of a design problem [14,15] seems to be a valuable approach that allows one to explicitly account for interactions between disciplines, avoiding typical problems of an omnicomprehensive approach.

The power of modern computers could induce an extensive exploitation of advanced computer-based methods, but they require a detailed knowledge of each domain that are not yet fixed in the initial stages of the design. This is especially true for the structural environment: the use of tools like finite element models (FEM) for the structural modelling may not be recommendable during the conceptual design phase. In particular, the use of detailed three-dimensional models could bias the results depending on arbitrarily assumed modeling choices, structural details, and optimization models. Furthermore, using a mix of simplified and complex schemes, for example, a three-dimensional CFD for aerodynamics and semi-empirical formulas for structures, seems to be inconsistent in terms of model accuracy.

Received 10 October 2008; revision received 20 October 2009; accepted for publication 19 December 2009.

*Assistant Professor, Dipartimento di Ingegneria Aerospaziale, Via La Masa 34; Giampiero.Bindolino@polimi.it.

†Professor, Dipartimento di Ingegneria Aerospaziale, Via La Masa 34; Gianluca.Ghiringhelli@polimi.it.

‡Associate Professor, Dipartimento di Ingegneria Aerospaziale, Via La Masa 34; Sergio.Ricci@polimi.it.

§Research Assistant, Dipartimento di Ingegneria Aerospaziale, Via La Masa 34; terraneo@aero.polimi.it.

According to these considerations, the paper deals with the problem of a suitable estimate of the wing-box weight in the presence of multidisciplinary constraints in the very early steps of aircraft design by means of an approach mixing well-known and affordable models with adequate optimization tools. The main scope is a procedure as fast and accurate as possible to conveniently assist the designer during the evaluation of different solutions in the very early steps of design as far as the structural design of the wing box is concerned, exploiting in the best way the link between analysis and design modules.

II. Procedure Overview

The work presented here lies in the framework of multilevel, multidisciplinary optimization. It is mainly based on the following remark: local design variables, such as the thickness of a panel or the section shape and the size of a stiffener, only indirectly affect the global behavior of the aircraft wing through a contribution to the stiffness of the related cross section. Thus, a multilevel decomposition has been envisaged to isolate several optimization problems and related design variables; the mutual relations are accounted for by means of adequate coupling functions that act as constraints in separate design loops. The flowchart in Fig. 1 describes the general layout of the procedure and its collocation inside the aircraft conceptual and preliminary design activities flow.

The present work represents the evolution of the procedure described in [16]; the level decomposition actually envisaged is based on design loops operating on three levels, each adopting a specific structural model coupled to an optimization algorithm:

1) The first level aims to grant a satisfactory global behavior of the wing by optimizing a one-dimensional model, based on beam approach; any available structural multidisciplinary analysis and optimization code can be used for this purpose, like MSC/NASTRAN [17] or Astros [18]; simplified models of the cross-sectional topology allow one to link physical design parameters to the cross-sectional properties; in this way, the availability of the structural mass estimate is obtained while also solving the problem of a consistent ratio among different cross-sectional stiffnesses without introducing further constraints.

2) Being available from the first level, the internal forces stressing the wing elements, a classical thin-walled beam cross-sectional analysis, coupled to a genetic optimizer, is used in the second level to fully design the wing box accounting for both sizing of the structural elements and choosing the topology of the cross-sectional and structural elements. Constraints are related to the satisfaction of local (allowable stresses, local and global stability of panels and stiffeners, etc.) and global requirements (cross-sectional stiffness properties defined by the first-level design).

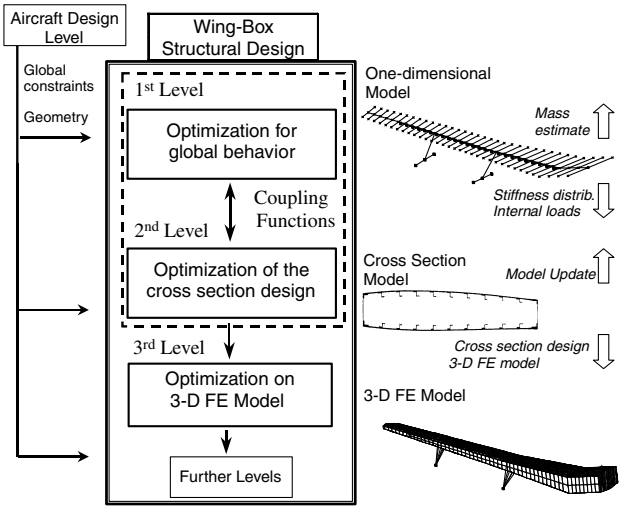

Fig. 1 Multilevel wing design procedure.

3) At last a three-dimensional FEM model, generated by means of data made available by previous levels, is planned to be used. It is not only devoted to the removal of problems left unsolved (e.g., stress concentration), cutout analysis, and the generation of data suitable for fatigue analysis, but it also guarantees a definitive verification of design requirements, for example, the actual deflection of the wing and its aeroelastic behavior.

The coupling functions between the first and second levels are defined in terms of the cross-sectional stiffness and internal force behavior along the wingspan. The inconsistency of some parameters after this phase, such as the shear center location, is always possible; thus, iterations between the first and second level should be required, especially when the first level shows great sensitivity to global aircraft performance, such as flutter speed, with respect to these parameters. The 3-D finite element models, produced by the third optimization level, combine available data so that they are not biased by either unnecessary nor arbitrary assumptions, with the geometry of the wing and both topological issues and physical sizing resulting from the second level.

The "bricks" used to build the present procedure are all well known to the engineering community; they are simply linked together by means of automatic interfaces with the goal of getting the most from each of them by the exploitation of modern computing techniques. This procedure has been developed independently but agrees with most of the requirements expressed in [19], such as a flexible interface with the aircraft designer, which may greatly affect the geometry and automatically generate geometric, structural, and aerodynamic models based on a minimal set of input data; the multidisciplinary structure, with the possibility of including relevant disciplines like aeroelasticity and active controls; the capability of evaluating alternative structural layouts; and the modularity of the software. Finally, the possibility of growth of the knowledge on the job, by learning from intermediate or more refined results to verify and, possibly, improve previous assumptions due to the multilevel approach adopted must be mentioned.

Because of the space limitation, the paper will focus on the first-level procedure only, leaving the detailed description of the remaining two levels to another paper.

III. First-Level Procedure for Wing-Box Weight Estimation

In this section the procedure suitable for the initial wing-box structural weight estimate, that coincides with the first level of the multilevel design procedure reported in Fig. 1, is presented. To face the specific problem of a quick weight prediction in conceptual aircraft design, reliable information is needed without fulfilling the whole design loop previously envisaged in [16], in which the weight estimate was available only at the end of the iteration on levels one and two. Because of these requirements, the first level has been changed with respect to the original formulation. Indeed, a schematic description of the cross-sectional properties [20,21] has been adopted, allowing significant advantage: the effective minimum mass optimization has been introduced, thanks to a suitable distribution of inertia forces and consistent cross-sectional relative values of stiffness (e.g., in-plane and out-of-plane bending stiffness, torsional stiffness).

A suitable layout of the first-level procedure is shown in Fig. 2. The procedure is basically a MATLAB® suite including tools for model generation as well specific interfaces to link external codes, such as the ones used for aerodynamic and structural analysis and optimization. Two external codes are adopted in the actual configuration of the procedure: an in-house-developed CFD code, used for the steady aerodynamic analyses, and MSC/NASTRAN, used for both structural analysis, including aeroelasticity, and optimization by means of the already available SOLUTION200. In this sense, the first-level procedure can be viewed as an MSC/NASTRAN preprocessor, representing a bridge between the Microsoft Office Excel sheets, typically used at the aircraft conceptual design phase, and the finite element models of increasing fidelity, adopted during the successive design phases. The designer is asked to supply a minimal

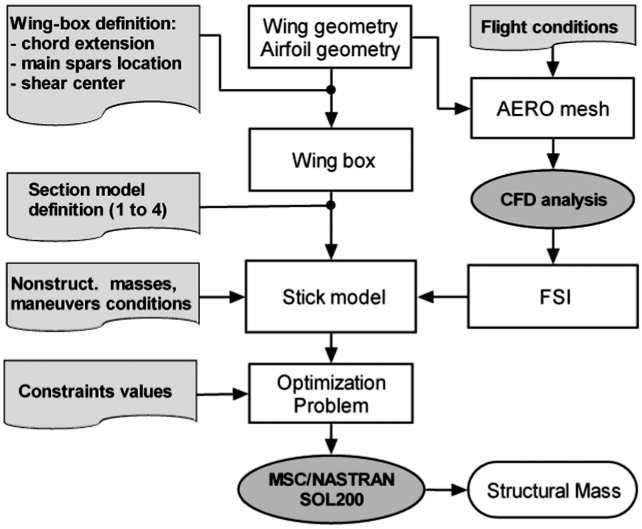

Fig. 2 First-level procedure layout.

set of data to accomplish the following steps: the definition of the structural model starting from the available geometry data describing the wing, the selection of the load conditions used for the wing-box sizing and weight determination. and the definition of the optimization model. In the following paragraphs, a brief description of each step is reported.

The structural model is determined by defining the part of the actual wing occupied by the wing box. First the external wing geometry is determined using the relevant data already known at this stage, such as span, chord distribution, swept angle, and adopted airfoils. Then, the wing-box geometry is extracted by imposing its chordwise extension, that is, the position of the front and rear spar, allowing for the calculation of the internal space available for fuel. Finally, the stick model of the wing box is generated and the nonstructural masses, coming from statistical-based approaches commonly adopted during the conceptual design phase, are introduced as distributed or nodal masses. This whole phase is managed in a graphical environment implemented using MATLAB and sketched in Fig. 3.

Once the structural model has been defined, the load conditions must be applied. They can be selected on the basis of an analysis of the flight and center of gravity envelopes and an accounting of regulations. The aerodynamic loads are evaluated by means of appropriate CFD codes and automatically applied to the stick model, whereas the inertia reliefs are computed by applying the acceleration levels due to the considered maneuvers.

Finally, as a last step, the optimization model has to be defined. It requires the definition of a usable objective function, as well as the definition of appropriate design variables and constraint functions. It must be underlined that, even if in principle the procedure can be linked to any external structural analysis and optimization code, in the actual version it is based on the use of an off-the-shelf code like MSC/NASTRAN, a de facto standard for the aerospace industry. Then, each choice made in the definition of the optimization problem has to be compatible with the capabilities offered by this code. The structural model is represented by a stick model, meaning a finite element model obtained using bidimensional elements like beams. This implies that the design variables are related to the section properties of the beams, assuming that the material properties and the wing geometry are kept constant during the optimization loop (no shape optimization). Nevertheless, by taking advantage of the DEQATN cards available in MSC/NASTRAN [17], which allows one to introduce user-defined relations between external design variables and finite element model properties, it is possible to conceive of any kind of wing section by defining the appropriate structural section model. Indeed, the section model represents the link between the physical wing section properties and the ones synthesized as beam properties: four section models are now available in the first-level procedure. Finally, different kinds of constraint functions can be considered during the optimization, including ones related to the aeroelastic behavior of the wing. The objective function is easily represented by the total structural weight.

The next subsections report in detail the most significant elements of the first-level wing-box design and optimization procedure that is simply summarized here, whereas no specific details related to the analysis modules and algorithms are reported. Indeed, by adopting MSC/NASTRAN as the structural and optimization solver, all kinds of analysis capabilities are already available and well known to the aerospace engineering community. For further details, the reader can refer to the MSC/NASTRAN official documentation [17,22].

IV. Structural Model

The first-level procedure exploits a beam model of the wing suitable to be analyzed and optimized by MSC/NASTRAN SOL200, taking advantage of all the static, dynamic, and aeoroelastic analysis capabilities already available in this very comprehensive multidisciplinary analysis code. As already introduced, the beam model is automatically generated from a reduced set of geometric wing data (planform wing, airfoils, aerodynamic twist, etc.; information that can be assumed to be fully available at this stage of the project) with very few further assumptions about the topology of the wing box, for example, the front and rear spar position, the location of shear center of the cross section, and the ribs pitch. In the framework of a one-dimensional approach, this allows an approximate but complete description of both the static and dynamic behavior of the wing when cross sections exhibit negligible coupling between internal forces. A nominal "average material" concept is used to link geometrical data to cross-sectional stiffness properties with an approach suitable for a metallic homogeneous design. In the case of composite technology, exploitation of a more complete beam model would be necessary: a less trivial evaluation of the equivalent averaged material is needed in this case to link geometric data to stiffness and mass properties. The reference line used for the beam model connects the centers of the wing box at relevant stations: they are evaluated by simply using geometry data, while the position of the shear center could be

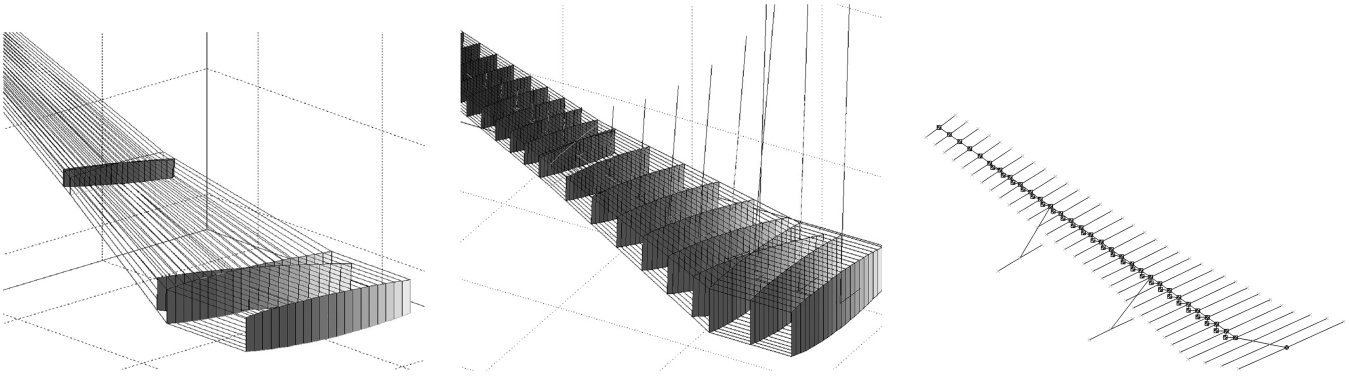

Fig. 3 From wing geometry to wing-box first-level finite element mesh.

updated after a second-level run, if needed. Nonstructural masses are also generated and included in the model according to the following criteria. Secondary structures and plants weights are predicted by using semi-empirical approaches or statistical formulas [1,7] that can be assumed to be still applicable, even in the case of unconventional aircraft. The fuel distribution is evaluated by accounting for the available internal volume so that the wing is loaded with the fuel actually fitting the wing box: the remaining fuel is assumed to be fitted in the fuselage or in other aircraft parts. Finally, the engine masses, geometry, and thrust are assumed to be available from general aircraft design.

A. Section Models and Design Variables

The physical properties of each cross section are estimated on the basis of an approximate description of the distribution of the material supporting axial and shear stresses, as in [21], in which a hexagonal cross section has been assumed; a simpler rectangular shape has been preferred for this work. Four different models, of increasing complexity, have been implemented to achieve a more and more effective understanding of the actual material distribution and to evaluate the effects on the total mass estimation; see Fig. 4. The models assume that an average thickness value is adequate to describe the geometry of the box. According to this choice three regions have been identified as fundamentals for each cross section: the webs (front and rear), the skin (upper and lower), and the skin stiffener region (modeled with an equivalent thickness only reacting to axial forces). Coefficients, relating the section geometry to the beam section properties by means of the design variables and the mechanical properties of an equivalent material, are analytically computed once the geometry of the beam cross sections has been obtained by intersecting a plane normal to the reference axis with the geometric model of the outer skin.

1. Model 1

Two design variables for every section have been considered. The thickness of the webs and skins are condensed in a single value representing the equivalent torsion box and contributing to bending properties; the remaining assessment is the equivalent axial thickness of the stiffeners.

2. Model 2

To better evaluate the true stiffness bending requirements, in-plane and out-of-plane of the wing, the second model retraces the preceding one by considering web and skin independent thicknesses for a total of three variables for every section. The equations to evaluate the beam cross section A, principal inertia moments I_1 and I_2, and the torsional stiffness coefficient J of a rectangular cross section, implemented in MSC/NASTRAN as DEQATN cards, are as follows:

$$A(t_e, t_w, t_s, c, h) = 2 \cdot (t_s \cdot c + t_w \cdot h + t_e \cdot c) \tag{1}$$

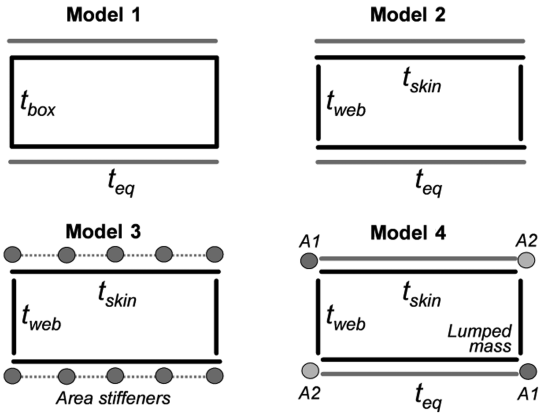

Fig. 4 Cross-sectional models and related design parameters.

$$I_1(t_e, t_w, t_s, c, h) = \left(\frac{t_w \cdot h \cdot c^2}{2} + \frac{(t_s + t_e) \cdot c^3 \cdot h \cdot c^2}{6}\right) \tag{2}$$

$$I_2(t_e, t_w, t_s, c, h) = \left(\frac{t_w \cdot h^3}{6} + \frac{(t_s + t_e) \cdot c \cdot h^2}{2}\right) \tag{3}$$

$$J_T(t_e, t_w, t_s, c, h, \Omega) = 2 \cdot \frac{\Omega^2 \cdot t_s \cdot t_w}{c \cdot t_w \cdot h \cdot t_s} \tag{4}$$

where c, h, and Ω are the chord, the averaged airfoil thickness, and the enclosed area of the wing box, respectively; furthermore, t_e is the equivalent thickness associated with the stiffeners, while t_w and t_s are the web and skin thicknesses, respectively. The first model is obtained by using a single variable for t_w and t_s, that is, $t_w = t_s$.

3. Model 3

To introduce the instability constraints of panels and stiffeners, a third material distribution variable has been introduced. Beyond t_w and t_s, another variable, A_s, is used. It represents the area of a single stiffener while the number of them/their distance is considered as a known parameter and settled at the beginning of the optimization, according to previous experience. The equations adopted to calculate the beam cross-sectional properties become

$$A(A_S, t_w, t_s, c, h, N) = 2 \cdot (t_s \cdot c + t_w \cdot h + A_S \cdot N) \tag{5}$$

$$I_1(A_S, t_w, t_s, c, h, D_2) = 2 \cdot \left(t_w \cdot h \cdot \frac{c^2}{4} + \frac{c^3 \cdot t_s}{12} + S_c \cdot D_2\right) \tag{6}$$

$$I_2(A_S, t_w, t_s, c, h) = 2 \cdot \left(\frac{t_w \cdot h^3}{12} + c \cdot \frac{h^2}{4} \cdot t_s + N \cdot A_s \cdot \frac{h^2}{4}\right) \tag{7}$$

$$J_T(t_w, t_s, c, h, \Omega) = 2 \cdot \frac{c^2 \cdot h^2 \cdot t_w \cdot t_s}{c \cdot t_w + h \cdot t_s} \tag{8}$$

where N is the stiffener number and D_2 is the summed squared distance of every A_s from neutral axis.

4. Model 4

To encompass the problems of unconventional wings, possibly requiring a significant rotation of cross-sectional principal axes to minimize bending stresses, as described in [20], two additional design variables can be added to the second model; independent additional flanges, of front and rear spars, are used. To obtain the desired effect, flanges are cross coupled: upper front with lower rear ones and upper rear with lower front ones.

The use of simplified cross-sectional shapes or a more precise one merely entails different calculations but small changes in stiffness coefficients. In any case it must be noted that this is only when starting from scratch; once a design is available from the second level, these coefficients can be improved to account for the actual design of each cross section.

The adoption of the equivalent thickness concept resembles the assumptions made in semi-analytical methods to define "bending masses" [7]. But in the present approach, the effects due to shear, torque, and instability can also be faced, even if by means of approximate models; this allows one to include considerations of either torsional stiffness or aeroelastic effects that cited approaches defer to subsequent design steps.

The availability of a reasonable estimate of the actual mass distribution of the primary structure enables the use of inertia forces in both static and dynamic analyses. It is evident that many data at this stage are not yet reliably available; they must then be assumed by means of a rational approach. Nevertheless, they may not be satisfactorily estimated; they will be upgraded as better data become available from the more detailed analyses carried out by the second design level. Sensitivity analyses can be exploited to verify this

problem: tests performed on this subject seem to minimize the relevance of this aspect.

B. Aerodynamic Models and Structural Model Loading

The aerodynamic models needed for load evaluation and aeroelastic simulations exploited, respectively, outside and inside the optimization loop are automatically generated. At present, a specific approach is used for each goal: a full potential formulation for load evaluation, implemented into an ah hoc developed aerodynamic code, and the doublet-lattice method for aeroelastic analysis and flutter constraint computation during the optimization phase, already available in MSC/NASTRAN. The full potential approach [23], solved by means of a boundary element method and extended to account for compressibility [24], is used to obtain the pressure distribution on the wing surface. It produces sets of forces applied to the beam model nodes by means of an interpolation code based on a proximity concept that are converted in nodal forces and directly applied to the MSC/NASTRAN mesh. As the aerodynamic code is an external and independent module, it could easily be substituted with other equivalent codes; for example, a 3-D Euler solver to bypass Mach limitations of the adopted approach. Loads are evaluated by iteratively trimming the aircraft until the needed aerodynamic resultant is obtained. An iterative procedure has been used also to evaluate loads on the deflected shape; it is known that the aerodynamic pressure evaluated on the undeflected geometry leads to internal loads higher than the actual one [19]. A soft coupling has been preferred between aerodynamics and statics; aerodynamic and structural boundary conditions are alternatively kept unchanged until the equilibrium at the deflected shape is attained.

The doublet-lattice method, used here because it is easily available in MSC/NASTRAN, allows for several aeroelastic analyses. In particular, the bidimensional aerodynamic model is linked to the structure by means of 3-D splines to supply adequate boundary conditions for the unsteady aerodynamic analysis.

V. Optimization Model

The structural model is coupled with an optimization model that, currently, allows MSC/NASTRAN SOL200 to pursue a minimum mass design by using the previously introduced section parameters as design variables. Design variables are linked to beam properties by means of coefficients evaluated according to the cross-sectional idealization adopted. Any structural response can be constrained during the optimization process: typical constraints refer to stresses, displacements and rotations, flutter speed, etc. According to the approach philosophy, only global requirements should be used as optimization constraints during the first level of design. Global stiffness constraints could be introduced in terms of tip displacement and rotation, as found in the literature, but a rational approach could be more useful (e.g., a minimum aileron effectiveness, to account for the aeroelastic effects of a swept wing, or the flutter clearance in the whole flight envelope) as described in Sec. V.A.2. Nevertheless, to limit the need for iteration between the first and second levels, it is very useful to introduce constraints on stresses as well. In this way, stresses due to bending are bounded using standard MSC/NASTRAN constraints (expressed in terms of the maximum axial stress in four points on the section); shear stresses, due to transversal loads and torque moment, are introduced by means of approximate theoretical equations. In the same framework, an approximated evaluation of the instability of stiffeners and panels could be introduced by simplified analytical functions, for example, Euler's formula. All these so-called special optimization constraints will be described in Sec. V.A.

The optimization strategy requires some remarks: static constraints can usually be profitably activated from the procedure start, whereas other constraints, in particular one on the flutter speed, can be conveniently activated later.

The adopted optimization code, that is, MSC/NASTRAN, suffers from a known restriction related to the single-model optimization: once the structural model is defined, it would be very useful to account for different sets and nonstructural masses, for example, to encompass inertia relief variable with flight configurations, either fully or partially filled tanks, empty tanks, or different kinds of constraints. To bypass this limitation in the case of multimodel optimization, the OPTIMUS code by NOESIS [25] has been used in place of MSC/NASTRAN to analyze two mass configurations during the same optimization run. It is slower than MSC/NASTRAN because of the use of finite differentiation to provide derivatives, but it is able to consider different finite element models at the same time.

A. Special Optimization Constraints

To introduce unconventional constraints, a direct writing of equations depending on design variables, user-provided coefficients, and analysis results has been exploited. Using this feature the constraints on the shear stress, the aileron effectiveness response, and the instability safety margins have been implemented.

1. *Approximated Shear Stresses*

The approximated equations used to obtain response in terms of shear stress in wing-box panels are related to the monocoque theory; assuming shear forces applied to the shear center and the geometry related to the principal axes, we can write the approximated equations for skin and web panel shear stresses:

$$\tau_w = \frac{|M_t|}{2 \cdot \Omega \cdot t} + \frac{|T_2|}{2 \cdot h \cdot t} + k \cdot \frac{|T_1|}{2 \cdot c \cdot t} \tag{9}$$

$$\tau_s = \frac{|M_t|}{2 \cdot \Omega \cdot t} + \frac{|T_1|}{2 \cdot h \cdot t} + k \cdot \frac{|T_2|}{2 \cdot c \cdot t} \tag{10}$$

where t is the panel thickness; c, h, and Ω are the chord, the height, and the enclosed area of the cross section, respectively; and M_t, T_1, and T_2 are the internal forces (torque and shear forces along principal axes). The last term in these equations is related to the shear flow on panels due to transverse shear loads: a $k = 0.5$ factor has been used.

2. *Aileron Effectiveness*

The incremental loads due to the aileron maneuver entails a change in airfoil attitudes and lifting forces; this load system attains a steady equilibrium in the case of no divergence. In a back swept wing, a reduction in lifting forces takes place, due to the wing bending, so that the aileron effectiveness decreases (washout effect). The roll effectiveness can be evaluated as follows:

$$\eta = 1 - \frac{\Delta M_{\text{Roll}}}{M_{\text{RollRigid}}} \tag{11}$$

where ΔM_{Roll} represents the reduction in the roll moment due to the structural flexibility. The effectiveness can be constrained, according to values for flexible wings at high speed. To compute the two terms in Eq. (11), incremental unit aileron loads are evaluated according to [26], so that the nominal rolling moment is directly available.

To estimate the change in rolling moment, the aileron loads are applied to the structural model in a specific subcase: using the strip theory, in which the wing is divided into strips associated with nodes and elements, the change in the aerodynamic attitude δ_i of ith strip is directly supplied by the structural solver and only depends on airfoil rotation. Then the change in the lifting force related to the ith strip is evaluated as follows:

$$\Delta L_i = q \cdot S_i \cdot (C_{L\alpha})_i \cdot \alpha_i \tag{12}$$

The total change in rolling moment is then straight computed by

$$\Delta M_{\text{Roll}} = \sum_i \Delta L_i \cdot b_i \tag{13}$$

where b_i is the distance of strip i with respect to the roll axis. The adoption of a constraint on roll effectiveness allows one to avoid arbitrary assumptions as far as constraints on the torsional stiffness

are concerned, for example, the one adopted in [21], which can exhibit a large as well as negligible influence on results just depending on numerical values that are not rationally defined.

3. Stiffener and Panel Instability

Simple analytical functions are implemented to evaluate panel and stiffener instability. The critical stress is compared to the maximum one in every section and the difference between them is constrained to be positive during the optimization phase. Euler's formula is used for the stiffeners:

$$\sigma_{\text{Scr}} = \frac{\pi^2 \cdot E \cdot I_s}{l^2 \cdot A_s} \tag{14}$$

where A_s and I_s are the area and moment of inertia, respectively; E is Young's modulus; and l is the rib pitch, kept as fixed during the optimization. Every stiffener in a wing section has the same area. Because the inertia of a section depends on the shape beyond the area, a Z section stiffeners has been supposed to be used; starting from the most common dimensions available on the market, a trend of the inertia/area ratio has been defined. This curve is a function of the area itself, and so the inertia presents a second-order polynomial behavior. Different shapes have been evaluated too, for example, C-, T-, and I-shaped stiffeners, but they exhibit small differences in their inertial/area ratio and so they were no longer considered.

The instability of panels is calculated by

$$\sigma_{\text{Pcr}} = \frac{\pi^2 \cdot E \cdot k_c}{12 \cdot (1 - \nu^2)} \cdot \left(\frac{t}{b}\right)^2 \tag{15}$$

where t is the *equivalent* panel thickness, E and ν are Young's and Poisson's moduli, b is the stiffener pitch and k_c is a coefficient related to the t/b ratio. The trend of this value is derived by [26]. The instability analyses request the availability of the area and the step of the stiffeners in every section and can be implemented only using the third-wing cross-sectional model. The introduction of these limits allows one to recover all the main physical attitudes of the wing box and overrules in some cases the optimization algorithm logic that can originate the minimum mass mathematical solution without any engineering meaning.

4. Flutter Constraints

The structural optimization including the flutter constraint represented for a long time a challenge for aircraft designers. The approach based on the inclusion into the optimization problem of a specific constraint expressed in terms of flutter speed is, in many cases, plagued by the presence of mode switching and hump modes. The consequence is that, during the optimization loop, even for a small change in the design variables, a jump could appear among very different flutter speed values or coupled modes, making the inclusion of flutter constraint into the active constraint set really difficult and thereby slowing down the convergence speed of the optimization process. The choice adopted in the procedure presented here is to express the flutter constraint by means of a rejection curve applied to the so-called V–g plot, representing the aeroelastic damping versus the flight speed. The rejection curve is defined by the user by assigning, for a preselected number of modes, a set of flight speed values for which a minimum value for the aeroelastic damping is required (see Fig. 5). In this way, a flutter constraint is transformed into M_{md} constraints expressed as

$$(g_i / g_i^{\min}) - 1 \leq 0 \tag{16}$$

where M_{md} is the number of points used to define the rejection curve and $g^{\min}$ is the minimum damping requested for the ith speed value. Thanks to the possibility offered by SOLUTION 200 of MSC/NASTRAN [17] to consider as a constraint during the optimization phase any of the model responses or any combination of them by using the DRESP1 and DEQATN cards, the flutter constraint as rejection curve is very easy to be implemented.

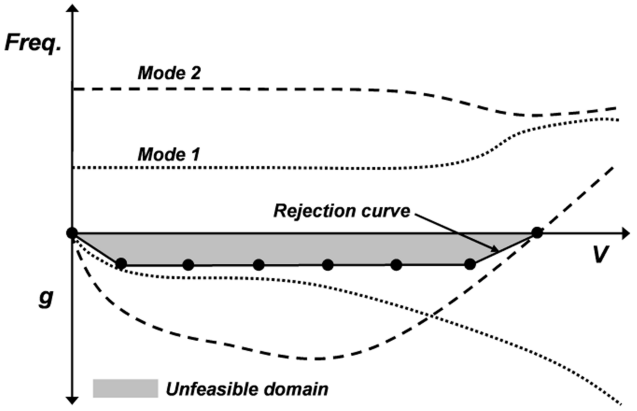

Fig. 5 Application of the flutter constraint by means of a V–g rejection curve.

B. Weight Estimation Corrections

From the conceptual point of view, the present approach keeps some relations with semi-empirical formulations: local effects are neglected by the adopted global model even if their relevance is known. According to this remark, a weight penalty can be introduced into the mass equation to account for the increase due to inspection cutouts; the correction coefficient has been assumed, according to remarks presented by [27], as $k_{\text{cutout}} = 5.0\%$ of the lower skin weight. Another important correction in the mass calculation comes from the fact that for aluminum alloy commonly used in aeronautics the maximum allowable compression stress is greater than maximum tension stress. The material models used are symmetrical and unable to appreciate this difference, and so some kind of correction, with the same approach adopted in [7], can be used and applied to structures mainly working under tension stresses.

VI. First Numerical Example: Boeing 747-100

The numerical example adopted here is represented by the weight estimation of the B747-100 wing box, depicted in Fig. 6, for which reference results are available in [1,28]. As the present approach was conceived for a tight integration with the global aircraft design process, a deep discussion of the approach features has been preferred to the presentation of results related to many cases. Some of the most relevant aircraft data are presented in Table 1, whereas in Table 2 the nonstructural masses included in the model are reported as evaluated in [7]. Airfoil geometry, needed to predict aerodynamic loads and to define the cross-sectional properties, has been gathered from [29]. Thirty-one beam elements linearly tapered between ends have been used to model the half-wing; constraints model the symmetry plane and supports at the fuselage connection. Stiffness coefficients have been computed accounting for the front and rear spars located at 17 and 58% of the aerodynamic chord at the root

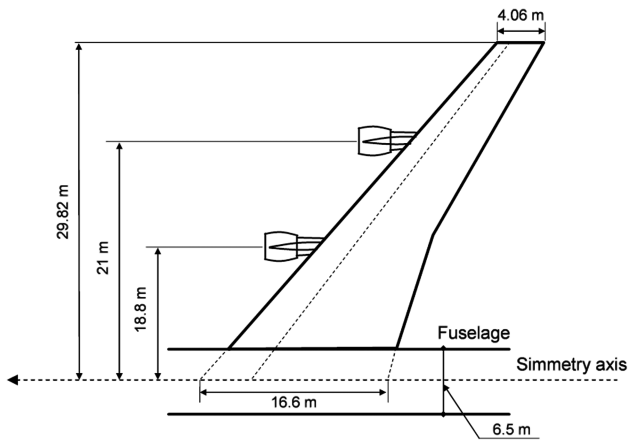

Fig. 6 B747-100 wing.

Table 1 B747-100: relevant data

Description	Value
Max takeoff weight	322,050 kg
Max zero fuel weight	238,815 kg
Max fuel weight (at MTOW)	83,235 kg
Wing surface	535.46 m^2
Wing span	59.64 m
Leading edge sweep	41 deg
Dihedral	7 deg
Wing–fuselage bulkhead	3.125 m
Design diving speed (velocity of dive)	286.6 m/s
Engine thrust (4x)	252 kN
Root section chord	14.55 m
Root section height	13.5%
Root section α	2.0 deg
Root section C_{box}/C	0.40
42% wing span chord	8.89 m
42% wing span height	8.0%
42% wing span α	1.0 deg
42% wing span C_{box}/C	0.47
Tip chord	4.06 m
Tip height	8.0%
Tip α	−4.7 deg
Tip C_{box}/C	0.40

station, whereas at the wing tip they are placed at 28 and 68% according to [30]. The reference axis has been aligned to the geometric center of the wing box. Masses related to leading- and trailing-edge aerodynamic elements and ribs, evaluated according to [7], have been distributed in term of weight per unit of area and lumped approximately on their center of gravity. Masses corresponding to the fuel have been distributed along the model up to 85% of the total wing span, according to the box surface. The elements related to the propulsion system (engines, nacelles, and pylons) have been placed according to available data (40 and 70% of the wing span, respectively).

A. Optimization Model

The main load condition is defined in [31] as a symmetric pull-up ($n = 2.5$) at the V_D and a 30,000 ft (9250 m) cruise altitude. Two configurations have been investigated: maximum takeoff weight (MTOW) with minimum fuel weight (83235 kg) and the maximum zero fuel weight with no fuel. These two cases represent the takeoff and landing of a mission with a full payload and give the possibility of evaluating the inertia relief contribution to the structural mass estimation. As far as the design speed, the value adopted in [20], that is, 229 m/s, seemed too low with respect to the actual one (268.6 m/s); thus, this latter value has been applied. The constraints summarized in Table 3 have been used. It is important to note that the structural mass estimated by the present method is strongly influenced by the axial stress limit adopted: the maximum stress listed in Table 3 comes straight from [31] and represents a minimum value able to consider all the aspects left out by the analysis, for example, fatigue life, instability, and stress concentration. An investigation of the sensitivity of the optimal design variable trend

Table 2 Nonstructural masses estimates

Description	Value for half-wing, kg
Ribs	830
L.E. fixed n.s.m.	1367
T.E. fixed n.s.m.	941
Triple slotted flap system	3392
Slats	810
Aileon and spoliers	435
Pylons (each)	1000
Engine and nacelle weight (each)	5128
Landing gear strengthener	255
Engine ribs strengthener (each)	274
Nonoptimal mass distribution	830

Table 3 B747-100: load conditions and design constraints

Load condition	Constraints
Symmetric pull up, $n = 2.5$	$\lvert\sigma_{max}\rvert < 233$ MPa $\lvert\tau_{max}\rvert < 116.6$ MPa
Aileron maneuver	$\eta > 52.5\%$ (at 250 kt)
Flutter clearance	$V_{Flutter} > 350$ m/s

due to the modification of this parameter is described in Sec. VII.C. The aileron effectiveness constraint was defined according to Boeing documentation [32] that refers to a 52.5% effectiveness at the maximum speed for the external aileron usage; finally, flutter clearance, with respect to the diving speed, has been obtained by rejecting damping greater than 0.01 up to 300 m/s and positive damping values for 320 m/s for the first eight deformable Eigenmodes. Only for the third cross-sectional model were local stability constraints included. An equivalent material was used by referring to the average values for aluminum alloys adopted in [7] showing $\rho = 2800$ kg/m^3, $E = 70$ GPa, and $G = 27$ GPa. The structural volume was used as an objective function to avoid problems on the convergence check in presence of prevailing and constant nonstructural masses.

B. Aeroelastic Load Evaluation

The change in the out-of-plane bending due to the modifications in the behavior of aerodynamic forces along the wingspan due to the structural deflection is well known. The introduction of aeroelastic load evaluation in the optimization cycle was performed by an iterative loop on aerodynamic trim and structural optimization: forces are derived by the rigid structure configuration and a preliminary optimization calculus is made; with the first attempt stiffnesses just found, an aeroelastic coupling is solved and the new loads, to use in a second-attempt optimization, are estimated. The procedure stops when the stiffness difference between two consecutive iterations falls under a user-defined limit. It is interesting to observe the behavior of structural responses in this loop: in Table 4 the trend of the wing-box mass, tip displacement, and tip change in attitude are depicted with respect to the load cycle number; it is possible to appreciate that, if the procedure stopped after the first iteration, it would be able to capture 99.9% of the final effects.

This approach supports a further remark about the shortening of the aeroelastic load evaluation procedure previously addressed: the changes in mass between one optimization iteration and the next one can easily exhibit the same magnitude of changes in loads, making it useless to search for very accurate load results at every step.

VII. Optimization Results

Numerous investigations were exploited to understand the different aspects concerning the optimization results: at first a comparison between the section models was made; after that the progressive introduction of constraints was evaluated using the same structural box scheme; finally the influence of maximum stress level change was investigated. The study of the sensitivity to the shear center position is reported here, whereas the evaluation of the modifications of the variable behavior due to aeroelastic static load introduction and different fuel configurations was left to the end.

Table 4 Aeroelastic procedure: parameters stabilization

Cycle	Total mass, kg	Tip deflection, m	Tip rotation, rad
0	76,009	3.519	−7.975e − 2
1	74,274	2.989	−6.367e − 2
2	74,272	2.997	−6.382e − 2
3	74,255	2.988	−6.358e − 2
4	74,253	2.990	−6.364e − 2
5	74,250	2.990	−6.363e − 2

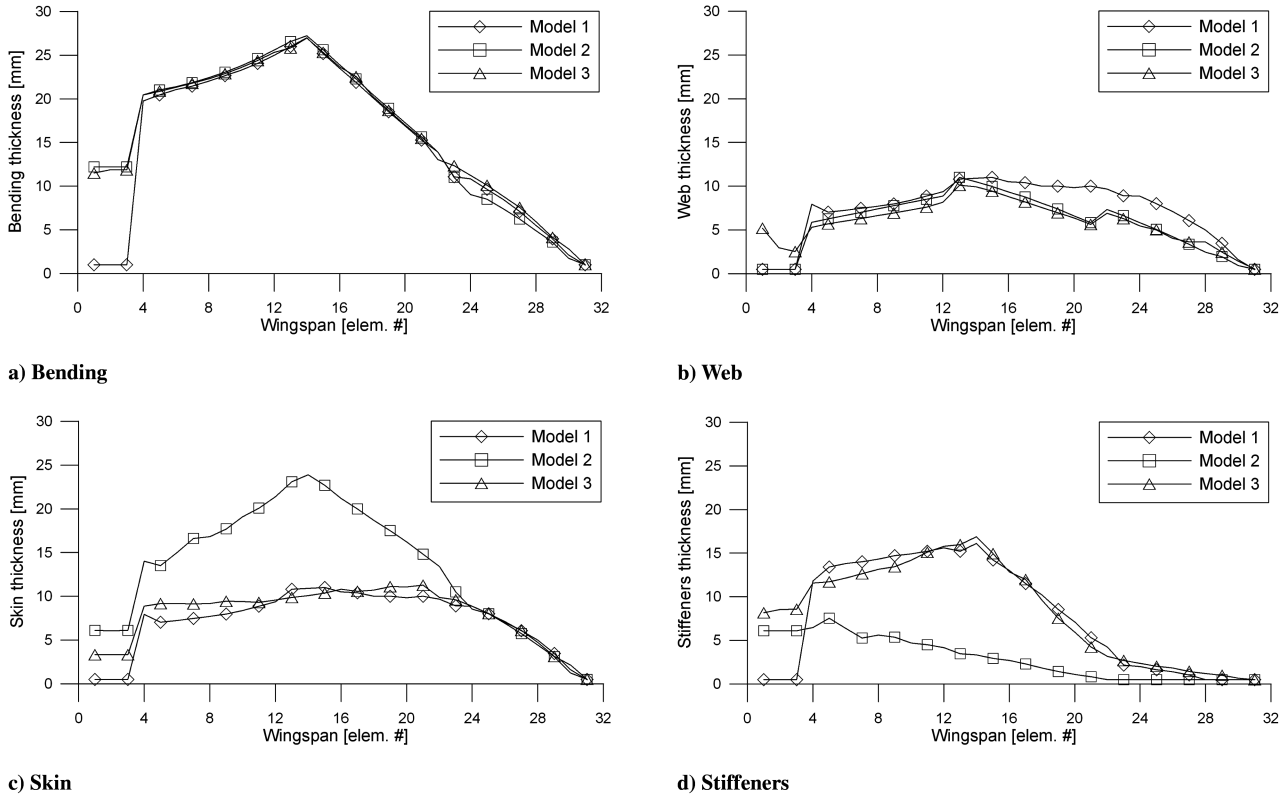

Fig. 7 Optimal design variable trend comparison for different section models.

A. Influence of Different Section Models

The first set of results is devoted to the discussion of the effects of the box model choice, with fixed design requirements, on both the estimate of the box-wing mass and the mass and stiffness distributions along the span. The constraints used are stress, flutter clearance, and aileron effectiveness. The comparison is exploited for MTOW configuration. Although the three structural models exhibit the same structural weight, the scatter is below 1% so that results are not presented; great differences are shown in the variable distribution along the wing span. The trend of the design variables, that is, the

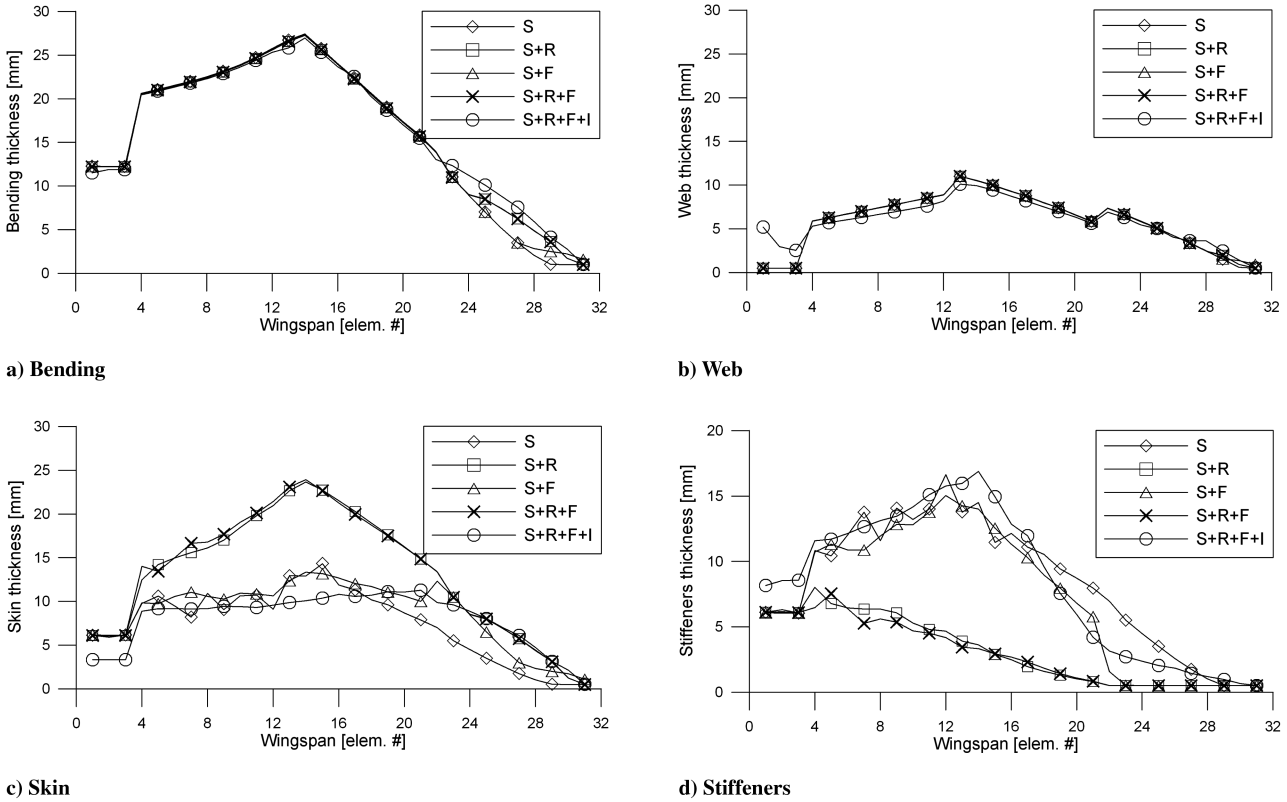

Fig. 8 Optimal design variable trend comparison for different constraints introduction.

Table 5 Results comparison

Case no.	Mass, kg	Mass, kg	Difference, %	Difference, %
	M_{Struct}	M_{Outwing}	M_{Struct}	M_{Outwing}
1	12,725	11,259	−0.72	−0.85
2	12,825	11,364	0.06	+0.07
3	12,749	11,287	−0.53	−0.61
4	12,817	11,356	——	——
5	12,746	11,320	−0.55	−0.32
4 +5%	13,058	11,583	1.88	+2.00
4 −5%	12,632	11,163	−1.44	−1.70

total equivalent thickness of material supporting axial loads and the thickness of the webs and skins, and the equivalent thickness of stiffeners are shown in Fig. 7. The solutions found by the three models are different, especially in the outer sections. The first model increases the whole box thickness to reach the needed torsional stiffness but uses more material than necessary for the webs; the result is an overestimation of the spar structural weight. The second model moves mass from the stiffeners to the wing panels (the stiffener equivalent thickness reaches the low limit) and the skin thickness is set to simultaneously satisfy the bending and torsion requirements. This strategy obtains a stiffer wing with equal weight but the result is, in engineering terms, meaningless: the elimination of the stiffeners originates panels that are too large, and so likely subject to instability; then the structural weight may be underestimated. The third section model seems to be the most reliable one: it exploits all the physical behavior of the wing and it is not affected by the problems of the earlier models. On the other hand, it requires a specific optimization strategy not available in MSC/NASTRAN and takes longer computational time. These troubles limit the effective use of this methodology in the conceptual design phase.

B. Influence of Optimization Strategy

The second set of results is aimed at the discussion of the effects of the optimization strategy, that is, of the possible choices available to the engineer for the constraint set definition. The following cases are discussed: 1) $n = 2.5$ pull-up maneuver with stress constraints (S), 2) case 1 plus aileron effectiveness constraint ($S + R$), 3) case 1 plus flutter clearance constraint ($S + F$), 4) case 2 plus flutter clearance constraint ($S + R + F$), and 5) case 4 plus instability constraint, obtained by a third model strategy ($S + R + F + I$).

The trend of optimal equivalent variables (expressed in millimeters) versus wing span, with a section model 2 strategy, is depicted in Fig. 8. The comparison allows one to understand how requirements on twist determine the distribution of mass and the stiffness properties along the wingspan: the simplest stress sizing leads to a thickness distribution regularly decreasing in the outer part of the wing. This allows one to keep the maximum axial stress on the bound value (until the technological bound on design variable is attained). The wing is, however, too weak under torsional loads and the addition of the stiffness requirement on aileron effectiveness moves thickness from axial to torsional purposes; note that the total thickness remains almost unchanged up to 60% of the half-span whereas an increase of box thickness is needed in the outer part. The further introduction of flutter requirement again entails the shift of material from axial to torsional purposes. In this process the out-of-plane bending stiffness is almost unaffected by the presence of roll and flutter constraints, whereas the introduction of a roll effectiveness constraint led to higher torsional stiffness in the inner portion of the wing. The presence of discontinuities in the inner span of stiffeners/skin thicknesses is due to a model ambiguity: they are absolutely equivalent for the optimizer that sometimes mixes up them; this situation can be easily singled out by noting that the bending thickness, that is, the sum of the two terms, exhibits a regular behavior. Especially in case 1, the lack of constraints on torsional stiffness and the presence of weak shear stresses lead the optimizer to find the axial resistance more advantageous. Thus, stiffeners and skin thickness were used indifferently to generate the necessary bending stiffness, with no regard to shear stresses. The introduction of global requirements, such as aileron effectiveness, brings to light the need for higher wing-box torsional stiffness. In the cross-sectional model, this inertia parameter is affected only by the thickness of webs and skins and the optimization algorithm prefers to move mass from

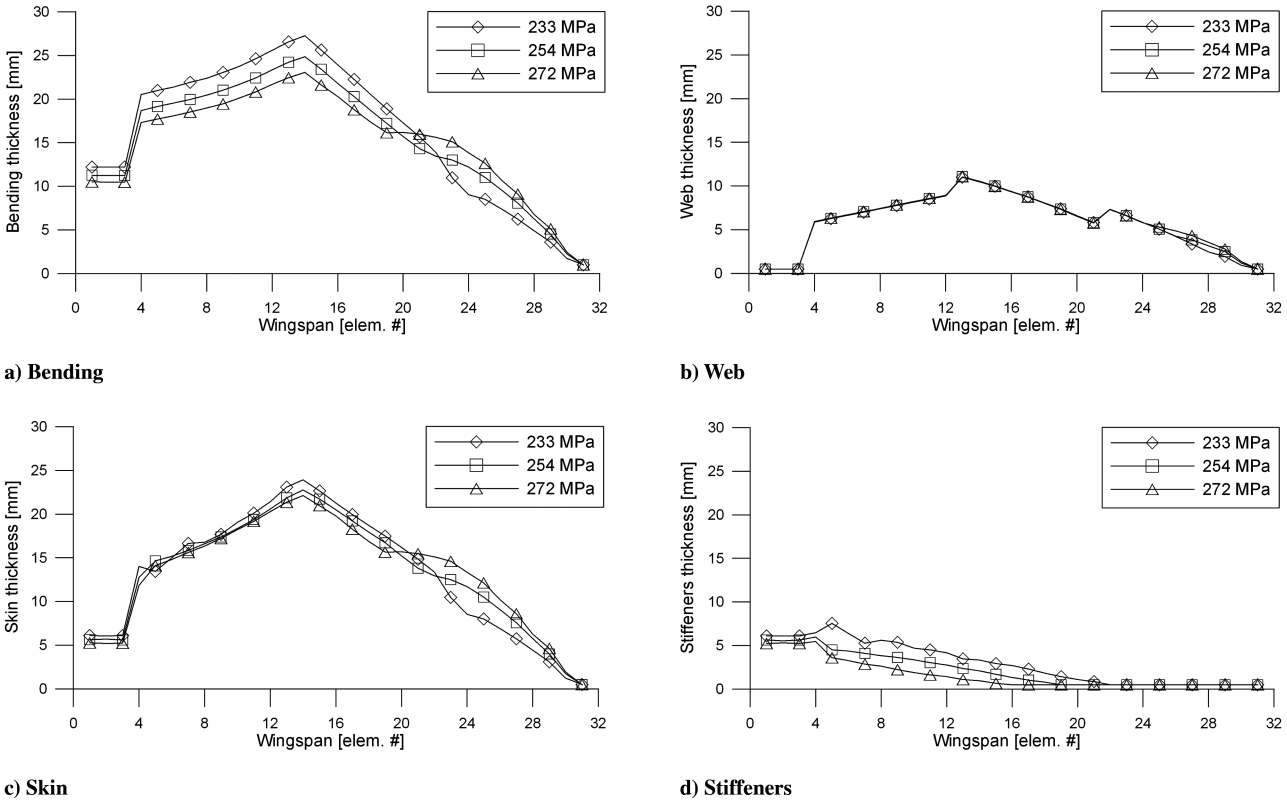

Fig. 9 Optimal design variables trend comparison for different maximum allowable stresses.

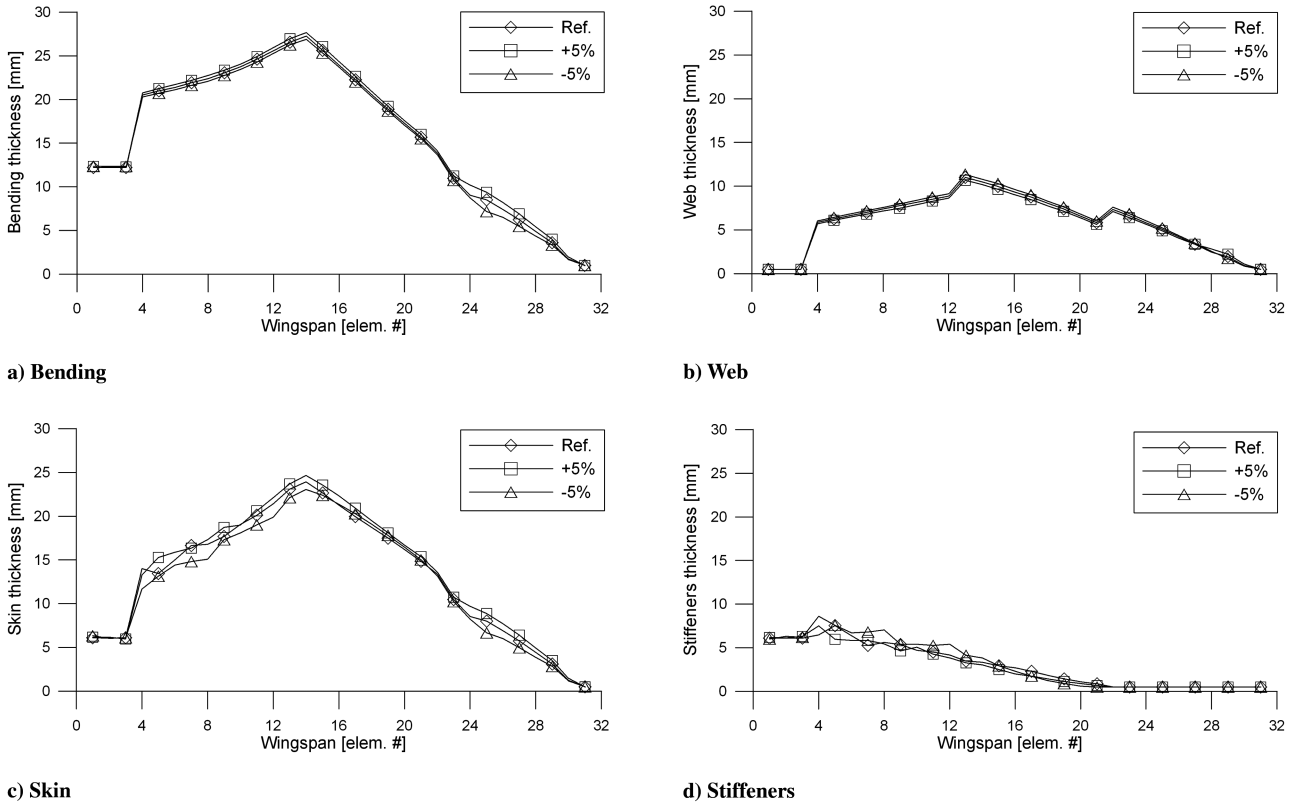

Fig. 10 Effects of different shear center positions comparison.

stiffeners to the torsion box: this choice is underlined by Fig. 8d, in which it is possible to see the value of the variable dropping to the technological minimum (0.5 mm). In case 5 this effect is not present because the instability constraints prevent the optimizer from doing this: in fact, the reduction in area generates unstable stiffeners and unfeasible solutions.

The results obtained in the four cases are very similar in term of mass, as one can appreciate in Table 5, in which M_{Struct} indicates the wing-box mass of the whole wing, then including the box in the fuselage, while M_{Outwing} is the portion of wing-box mass concerning the cantilever part. It must be noted that the knowledge of the material distribution along the wingspan allows one to estimate relevant information, for example, the longitudinal c.g. position of the wing box as well as the contribution to inertia around the roll axis.

C. Influence of Maximum Allowable Stress Values

From the optimizer point of view, the wing seems to be divided into two parts: the maximum allowable stress is the active constraint in the first one, approximately spanning from the root to two-thirds of the wingspan, whereas in the second one the optimal design is driven by stiffness constraints. This consideration is clearer if the trend of input variables is investigated against the maximum allowable stress variation. In Fig. 9a, which represents the equivalent bending thickness, it is possible to appreciate how an increment of the maximum allowable stress reduces the part of the wing for which the design is defined by static load, so increasing the influence of flutter and roll boundaries; not only the total weight of the wing is diminished but the whole variables trend is changed.

The algorithm logic is practically the same in every case: in the inner section the most important request to be satisfied is the out-of-plane sectional inertia, and this demand is assured to scale conveniently the variable values; in the tip zone the inputs have to guarantee a correct global behavior of the structure, and so they increase themselves to compensate for the stiffness loss due to the root part mass reduction.

D. Influence of Shear Center Position

Some further tests have been carried out to verify the sensitivity of the results with respect to the shear center position: the shear centers have been moved forward and backward in terms of the percentage of the box local chord (±5%). A comparison of the reference optimization results shows that the influence on the weight estimation can at first be considered time negligible, as one can appreciate from the two last rows presented in Table 5. All the cited cases produced almost the same prediction: simply a different use of the same amount of material is envisaged (Fig. 10). This result suggests

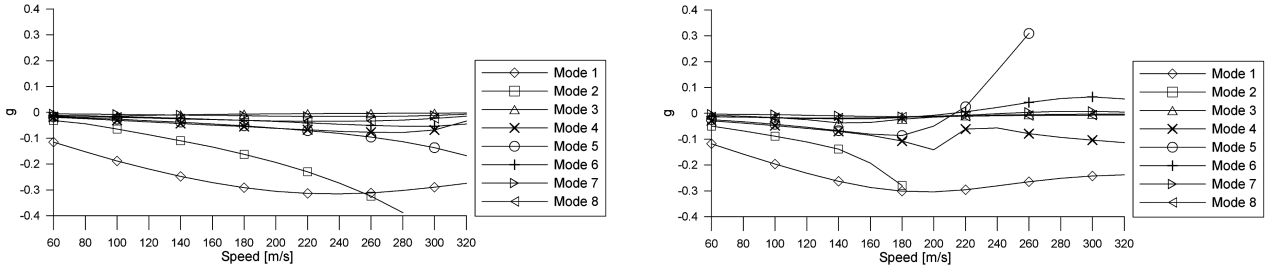

Fig. 11 *V–g* plots with and without flutter constraint.

Table 6 Aeroelastic results comparison

Case no.	Mass, kg	Mass, kg	Difference, %	Difference, %
	M_{Struct}	M_{Outwing}	M_{Struct}	M_{Outwing}
1	10,966	9603	−6.36	−7.36
2	11,712	10,367	+0.01	+0.01
3	10,868	9518	−7.20	−8.18
4	11,711	10,366	——	——
5	11,864	10,514	+1.31	+1.43

that in a preliminary phase a "reasonable" collocation of the shear center could be enough to produce reliable mass predictions, even in the presence of aeroelastic constraints. The most significant change in stiffness behavior occurred in the case of a 5% afterward offset of the shear center: in this case a higher torsional stiffness in the outer portion of the wing has been required and obtained by further moving material from axial to torsion and increasing the panel thickness. Nonetheless, the total bending thickness is almost unaffected and the total box weight remains very close to other results. A dual effect of the preceding one is obtained for a −5% offset: the torsional requirement is less restrictive and so the material needed near the tip decreases. Results produced by the procedure are completed by classical V–g plots obtained from the model optimized without and with flutter constraints (Fig. 11).

E. Rigid Versus Aeroelastic Optimization

A comparison of the rigid and aeroelastic optimizations has been exploited too: the aerodynamic loads are not now evaluated on the undeformed shape but they are calculated by an iterative procedure accounting for the wing flexibility. The values obtained and the trend of optimization variables in the latter case is shown in Table 6 and Fig. 12, respectively. The reduced bending moment and the changed aerodynamic forces acting on the wing originates a solution lighter than the previous one, of about 9%, as well as a different behavior of stiffness distribution. Furthermore, the roll constraint becomes more important than the rigid case being active in all the outer section: the torsional stiffness is increased by higher web and skin thicknesses whereas the stiffener contribution is left at the minimum. Even with a large increment in the CPU time, the flexibility of the structure can be set aside only in a very preliminary phase of the study due to the great influence of this contribution on the final results, in terms of both total mass and variables trend.

F. Influence of Different Fuel Distributions

To account for the effects of fuel, the same aircraft configuration, but with no fuel in the tanks, has been considered. In this case the total lift is reduced but also the inertia relief is lower; furthermore, the dynamic aeroelastic behavior may be affected. Load distributions present a very similar behavior even if the effect of the concentrated mass representing fuel is neglected. The values of internal forces, bending torsion, and shear are lower in the new configuration flight, and so a lighter weight estimation is obtained (about −13%); furthermore, the distribution of mass along the span is very different and, near the tip, the optimal solution is stiffer to satisfy flutter constraint (Fig. 13). The results shown refer to section model 2 with all the constraints active. The presence of different optimal stiffness distributions suggests a multiple flight conditions approach, but the optimization tool of MSC/NASTRAN is not able to consider more models at the same time, even if the use of selectable lumped masses could be at hand. Thus, a commercial software, named OPTIMUS by NOESIS, has been used. In every case considered here, the same optimization strategy and parameters have been used. To investigate the influence of the optimization algorithm on the obtained results, some analyses with different starting points have been carried out to check the sensitivity of the approach to initial values: results show very small discrepancies, even if the convergence results vary slow, requiring 16, 69, 150, and 105 iterations for optimization cases 1–4, respectively.

The comparison with reference wing-mass prediction [1,7,28] is presented in Table 7 for the half-wing, whereas the actual value is derived from [7]. Data have been consistently reduced to the total box mass (MBOX), which represents the sum of outboard wing box, ribs, and nonstructural masses. The comparison shows a satisfactory agreement, despite the fact that some unavailable data have been

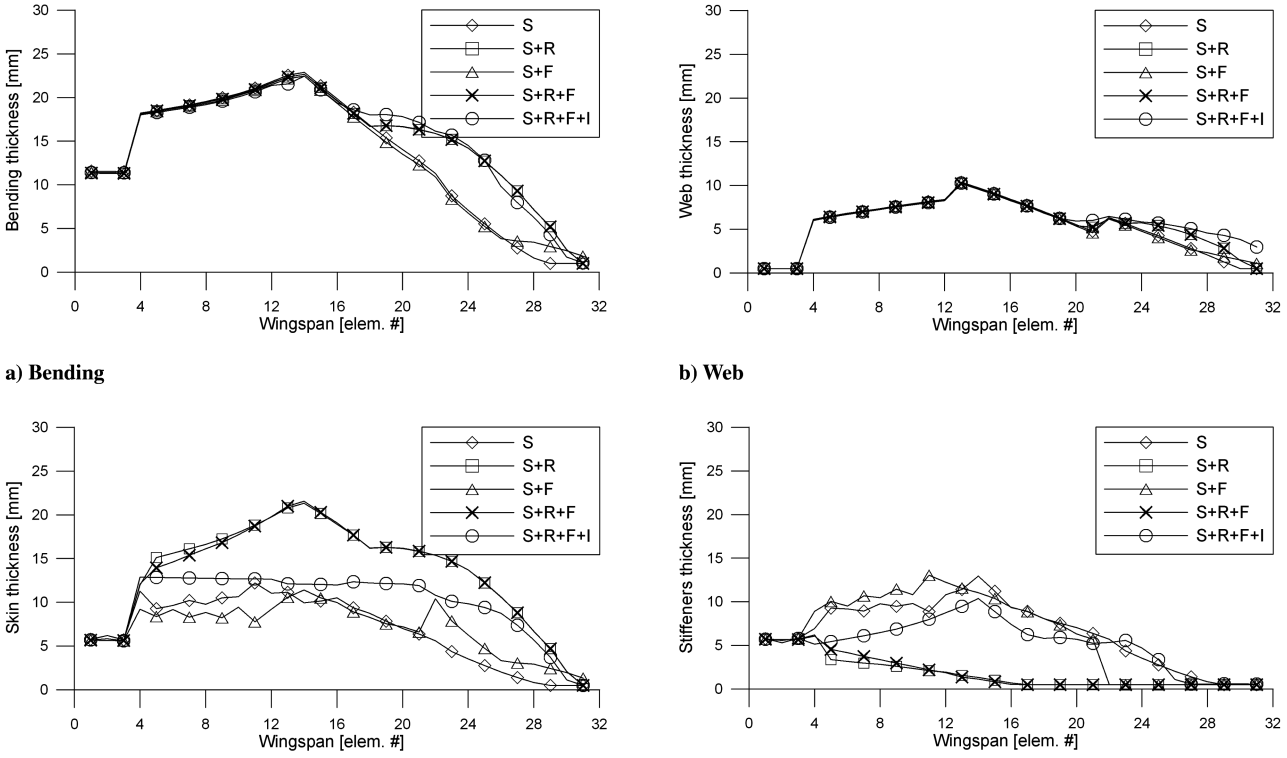

a) Bending **b) Web**

c) Skin **d) Stiffeners**

Fig. 12 Optimal design variable trends in aeroelastic configuration.

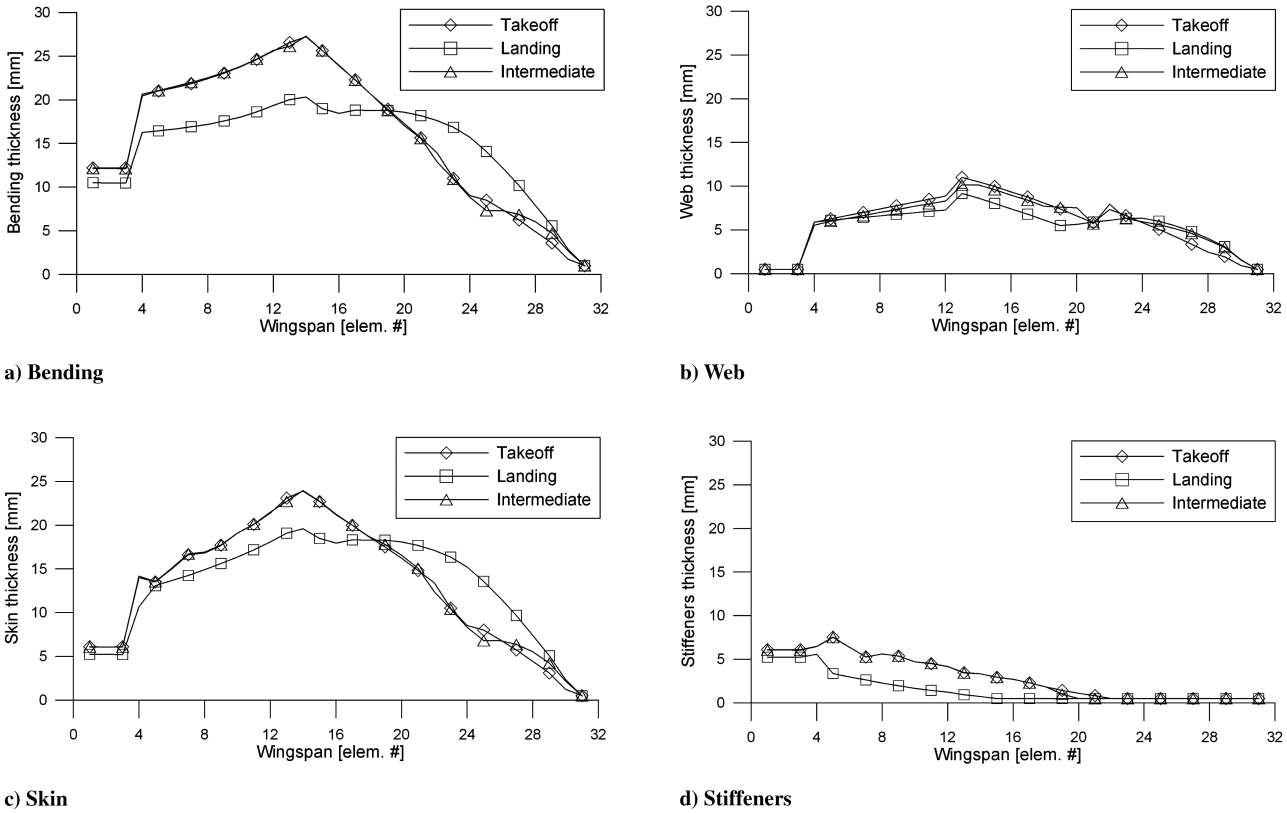

Fig. 13 Optimal design variable trends for different fuel configurations.

arbitrarily, but reasonably, assumed without further confirmation. As far as aeroelastic phenomena is concerned, only flutter and roll constraints have been used in this work, but other requirements can be added, for example, bounding stresses and accelerations due to gust response. Furthermore, the confidence in results could be increased by checking assumptions with the results coming from the design of each cross section. At the end of this work, partial and preliminary investigations have been exploited for the possibility of using composite materials technology. Slight modifications have been introduced in the structural beam definitions to introduce the possibility of working with different materials at the same time: the different technology used to build stiffeners and panels has been highlighted, differentiating their mechanical behavior. Using the lamination theory for a symmetric and balanced plate, an equivalent isotropic material has been calculated with $E = 67.2$ GPa, $G =$ 68.7 GPa, $\nu = 0.2$, and $\rho = 1900$ Kg/m^3 to use for webs and skin; for the stiffeners, a unidirectional laminate has instead been foreseen with $E = 200$ GPa, $G = 4$ GPa, $\nu = 0.2$, and the same density. Maximum axial stresses have been differentiated too: in the panels, the fiber orientations generate different stress status in the plies and, to consider the maximum one, an opportune reduction of the admissible stress has been accounted (adm = 445 MPa); in the stiffeners, the comparison has been directly made against the value in the literature (adm = 600 MPa). The maximum shear stress has been fixed to 250 MPa. The first results, coming from a model 2 strategy with roll and flutter constraints activated, show a reduction in mass of −29.6% (from 12,817 to 9018.8 Kg) as well as an increment of the torsional stiffness. Further analyses with a discrete input variable optimization strategy accounting for the number of plies is scheduled for an upcoming work.

Table 7 Comparison of weight estimations with reference data

Reference	Mass, kg	Difference , %
B747-100 wing	19,592.2	——
Torenbeek [7]	19,956.8	+1.86
Roskam [1]	19,580.5	−0.06
Macci [28]	19,260.5	−1.69
Present (rigid)	19,962.0	+1.89
Present (aeroelastic)	18,972.0	−3.17

VIII. Second Numerical Example: PrandtlPlane Configuration

Once reasonable results have been obtained with a conventional wing, such as one of B747-100, in comparison with data available from literature, the first-level procedure is applied to the nonconventional configuration based on the PrandtlPlane concept described in [33], which is characterized by a wing system composed of a lower forewing and an upper aftwing, joined at tip by a vertical bulkhead, as shown in Fig. 14). This configuration is, from the structural point of view, statically indeterminate; thus, the internal forces depend on the stiffness distribution too. In [34] it has been demonstrated that this architecture exhibits minimal induced drag, extending Prandtl

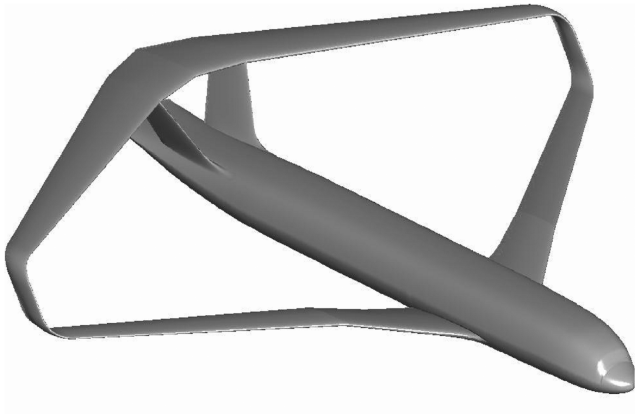

Fig. 14 PrandtlPlane configuration.

considerations to a swept wing box. The wings of the aircraft at hand are characterized by a high vertical gap obtained by supporting the aftwing with a double fin, allowing for a higher efficiency of the wing system. The aircraft lies in the class of very large commercial transport: the number of passengers, the gross weight, and the general size are similar to the Airbus 380 (the main properties are summarized in Table 8). The aircraft is pushed by four engines, two mounted on each wing, of the same class as the Airbus 380, with 300 kt maximum takeoff thrust.

A. Optimization Model

The wing box has been modeled with 37 elements in the forewing, 10 in the bulkhead, 36 in the aftwing; five elements model the fin and are linked to the wing with a rigid element. Nonstructural masses have been evaluated by using the same semi-empirical formulas already used for the preceding example. The resulting 21,000 kg have been distributed proportionally to chord distribution law. The obtained model is sketched in Fig. 15. The fuel mass has been distributed proportionally to the wing-box internal volume, assuming 85% of nominal volume and accounting for the maximum fuel quantity, which resulted in this condition being the heaviest one. Two load conditions have been considered: a cruise condition with static aeroelastic constraints expressed in terms of maximum tip deflection and torsion, and a pull-up maneuver under stress limits on both normal and shear stresses. Also in this case the structural weight is assumed as an objective function. The loads have been computed by means of the aerodynamic boundary elements method, whereas inertia relief has been accounted for by MSC/NASTRAN itself, thanks to the appropriate gravity load condition. The optimization constraints are summarized in Table 9. Two different sets of design variables have been considered for each case: the first one only accounts for axial and torsion thicknesses, whereas the second one also accounts for asymmetric spar flanges using model sections 2 and 4, respectively.

B. Optimization Results

Because of the uniqueness of the analyzed configuration, no available data are at our disposal from literature for the sake of comparison. Thus, general comments about the present method can be drawn. Two optimization runs have been performed, using section models 2 and 4 to define the beam element properties, allowing for symmetric and asymmetric spar flanges, respectively; the results in terms of total wing-box mass are summarized in Table 10. The minimum structural weight configuration has been found without any particular difficulty in 12 and 14 iterations, respectively. It is interesting to note the minimal stiffness/thickness zone located approximately at one-third of the wing span in both the forewing and aftwing (Fig. 16). This is due to the presence of a change in sign in the out-of-plane bending moment (the orientation of the local frame vertical direction lies approximately along the absolute reference vertical axis): as the in-plane bending moment on the contrary is always nonnull and due to a variable out-of-plane and in-plane bending moment ratio, the rotation of the cross-sectional principal axis is required to keep stresses below the limits. This is depicted in Figs. 17 and 18, in which these internal forces are plotted along

Table 8 PrandtlPlane: relevant data

Description	Value
Max takeoff weight	600,000 kg
Max fuel weight (at MTOW)	220,000 kg
Wing surface	811.0 m^2
Wing span	78.0 m
Leading-edge sweep forewing	38 deg
Leading-edge sweep aftwing	−23 deg
Fuselage diameter	8 m

Table 9 PrandtlPlane: load conditions and design constraints

Load condition	Constraints
Symmetric pull up, $n = 2.5$	$\lvert\sigma_{\max}\rvert < 233$ MPa $\lvert\tau_{\max}\rvert < 116.6$ MPa
Max tip displacement for $n = 1$	$\eta < 2$ m (at 250 kt)
Max tip rotation for $n = 1$	$\theta < 2$ deg (at 250 kt)

Table 10 PrandtlPlane: optimization results

Flanges	Iterations	Optimized mass, kg
Symmetric	12	54,025
Asymmetric	14	36,643

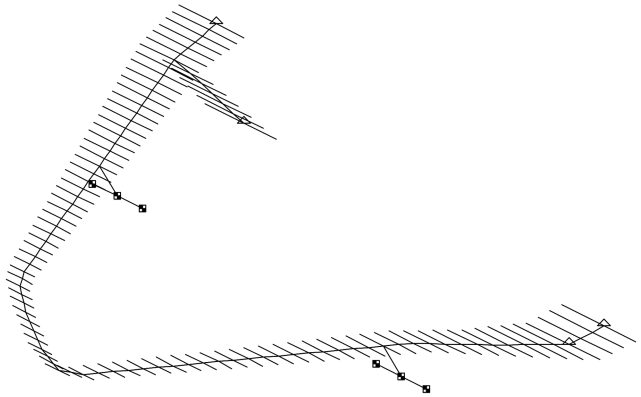

Fig. 15 PrandtlPlane first-level structural mesh.

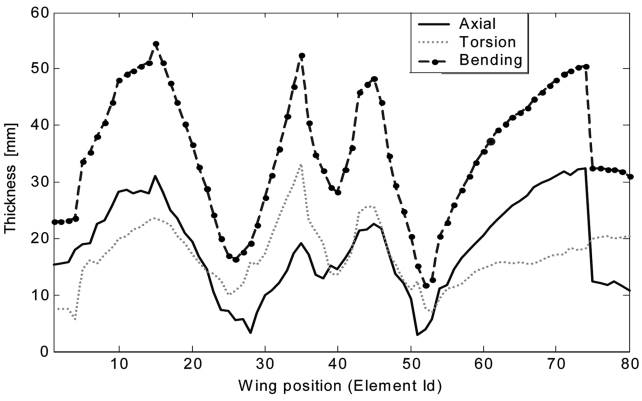

a)

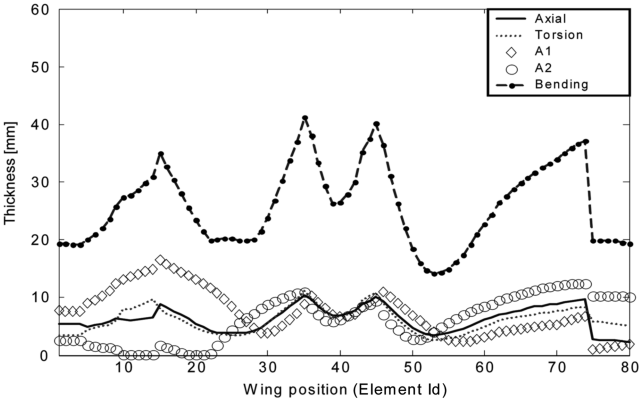

b)

Fig. 16 Effects on design variables due to the flange models: a) symmetric, and b) asymmetric.

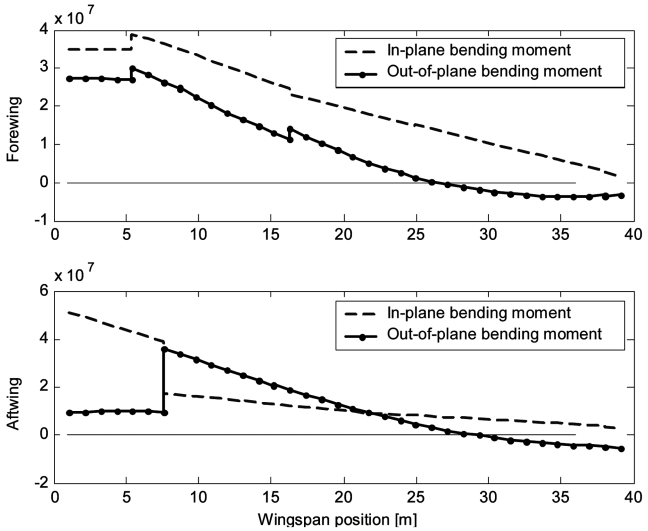

Fig. 17 Internal force distribution due to the flange models: symmetric.

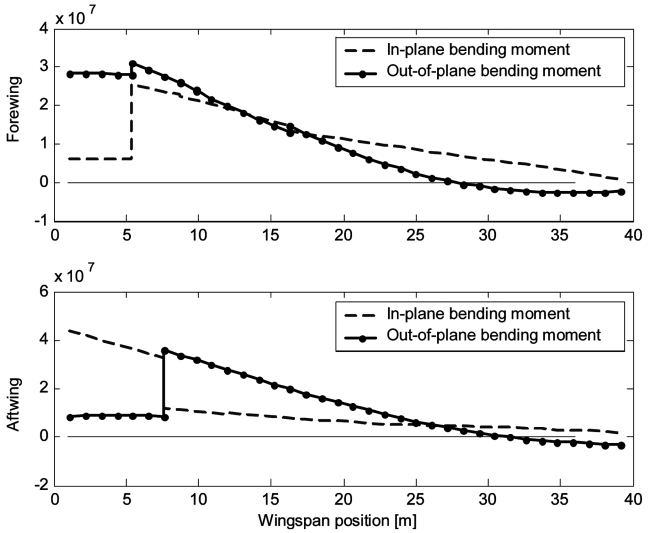

Fig. 18 Internal force distribution due to the flange models: asymmetric.

wingspan in the case of symmetric and asymmetric flanges. This effect is also dependent on the stiffness distribution due to the indeterminate structural layout in which the structural mass distribution greatly affects the internal forces. Nevertheless, the optimization module catches this requirement. It is evident that the orientation of the section principal axis is far from being constant along the wing; thus, its effects cannot be predicted by too-simplified structural models typically adopted during aircraft conceptual design, whereas it is very effective on the predicted wing mass. Indeed, in the approach presented here, the use of section model 4, in which two different design variables are used to define the asymmetric configuration of the spar flanges, guarantees a significant reduction of about 30% in the final optimal structural weight, as shown in Table 10.

IX. Conclusions

A procedure suitable for the preliminary estimation of inertia properties of the wing box of an aircraft is presented. The main features of the procedure are related to the capability of accounting for torsional and aeroelastic requirements, an easy interface to the initial sizing level, and the availability of information on the wing-box mass and on its distribution, as well as some other relevant inertia properties; furthermore, many kinds of constraints, ranging from stress/displacement constraints for static load conditions to flutter clearance and gust response, can be enforced. Adequate flexibility is granted to the designer that can include any number of load conditions, each together with specific constraints. The procedure is currently interfaced to a boundary element code, based on a potential approach, for the aerodynamic load evaluation and an interpolation module for the automatic loading of the structural model. The weight evaluation is entrusted to a commercial optimization code: the behavior of mass and stiffness is optimized to satisfy global requirements by exploiting simplified physical cross-sectional design variables, linked to them by means of geometric analytical coefficients.

The features of the presented approach have been extensively discussed for a large aircraft. The approach has been compared, at first, to classical semi-empirical methods for the estimation of the wing-box mass of a conventional liner showing a satisfactory agreement. Then, it has been successfully applied to the wing weight estimation of an unconventional aircraft, like the PrandtlPlane, showing a close wing configuration. Even in this case, the approach proposed has been able to find the minimum structural weight configuration, also taking into account the unusual stiffness distribution due to the undeterminate structural layout.

The main advantages of the proposed procedure can be summarized in the following statements. The procedure offers an easy interface to the initial aircraft sizing level, which supplies the main geometric parameters of the wing, and represents an efficient tool for the generation of structural and aerodynamic finite element models. The adoption of a well-established approach for the minimum structural weight estimation offers a practical alternative to the classical weight estimation tools, based on statistical data, in the case of unconventional aircraft configurations. The separation of the local variables from the general problem and the identification of the smallest number of variables able to catch the complete behavior of the problem at every optimization level avoids the need for calculating the sensitivity of the objective and constraints versus design variables that slightly affect them, thereby increasing the computational efficiency. The adoption of a multidisciplinary approach to the wing structural optimization problem starting from an aeroservoelastic standpoint allows one to easily introduce the active control systems in the first-level cycle to optimally design the control gains.

References

[1] Roskam, J., *Airplane Design*, Roskam Aviation and Engineering Corp., Lawrence, KS, 1986.

[2] *Introduction to Aircraft Weight Engineering*, Society of Allied Weight Engineers, Los Angeles, CA, 1996.

[3] Livne, E., "Aeroelasticity of Joined-Wing Airplane Configuration: Past Works and Future Challenges—A Survey," AIAA Paper 2001-1370, April 2001.

[4] Grandhi, R., Bharatram, G., and, V. B., V., "Multiobjective Optimization of Large Scale Structures," *AIAA Journal*, Vol. 31, No. 7, July 1993, pp. 1329–1337. doi:10.2514/3.11771

[5] Bhardwaj, M. K., "CFD/CSD Interaction Methodology for Aircraft Wings," Ph.D. Dissertation, Virginia Polytechnic Institute and State University, Blacksburg, VA, Oct. 1997

[6] Leoviriyakit, K., and Jameson, A., "Aero-Structural Wing Planform Optimization," AIAA Paper 2004-0029, Jan. 2004.

[7] Torenbeek, E., "Development and Application of a Comprehensive Design-Sensitive Weight Prediction Method for Wing Structures of Transport Category Aircraft," Delft University of Technology Tech. Rept. LR-693, Delft, The Netherlands, 1992.

[8] Sobieszczanski-Sobieski, J., and Haftka, R., "Multidisciplinary Aerospace Design Optimization: Survey of Recent Developments," *Structural and Multidisciplinary Optimization*, Vol. 14, No. 1, 1997, pp. 1–23. doi:10.1007/BF01197554

[9] Klimmek, T., Kiebling, F., and Honlinger, H., "Multidisciplinary Wing Optimization Using a Wing Box layout concept and Parametric Thickness Model," AIAA 2002-6757, Sept. 2002.

[10] Bernardini, G., and Mastroddi, F., "Multidisciplinary Design Optimization for the Preliminary Design of Aeronautical Configura-

tions," AIAA Paper 2004-1544, April 2004.
[11] Balling, R. J., and Sobieszczanski-Sobieski, J., "Optimization of Coupled Systems: A Critical Overview of Approaches," *AIAA Journal*, Vol. 34, No. 1, pp. 6–17. doi:10.2514/3.13015, Jan. 1996.
[12] Schuman, T., de Weck, O., and Sobieski, J., "Integrated System-Level Optimization for Concurrent Engineering with Parametric Subsystem Modeling," AIAA Paper 2005-2199, April 2005.
[13] Monell, D. W., and Piland, W. M., "Aerospace Systems Design in NASA's Collaborative Engineering Environment," International Astronautical Federation Paper 99.U.1.01, Oct. 1999.
[14] Sobieszczanski-Sobieski, J., James, B., and Dovi, A. R., "Structural Optimization by Multilevel Decomposition," *AIAA Journal*, Vol. 23, No. 11, pp. 1775–1782. doi:10.2514/3.9165, Nov. 1985.
[15] Schmit, L. A. Jr., and Ramanathan, R. K., "Multilevel Approach to Minimum Weight Design Including Buckling Constraints," *AIAA Journal*, Vol. 16, No. 2, pp. 97–104. doi:10.2514/3.60867, Feb. 1978.
[16] Ghiringhelli, G., and Ricci, S., "A Multi-Level Approach to Preliminary Optimization of a Wing Structure," *International Forum on Aeroelasticity and Structural Dynamics 2001*, Paper 090, June 2001.
[17] Moore, G., *MSC/NASTRAN—Design Sensitivity and Optimization*, The Macneal–Schwendler Corp., Los Angeles, CA, 1994.
[18] "ASTROS Ver. 10 Users Manual," Universal Analytics, Inc., Torrance, CA, 1993.
[19] Kelm, R., Lapple, M., and Grabietz, M., "Wing Primary Structure Weight Estimation of Transport Aircrafts in the Pre-Development Phase," Society of Allied Weight Engineers Paper 2283, May 1995.
[20] Hajela, P., and Chen, J., "Preliminary Weight Estimation of Conventional and Joined Wings Using Equivalent Beam Models," *Journal of Aircraft*, Vol. 25, No. 6, 1988, pp. 574–576. doi:10.2514/3.45625
[21] Gern, F., Naghshineh-Pour, A., Sulaeman, E., Kapania, R., and Haftka, R., "Flexible Wing Model for Structural Wing Sizing and Multidisciplinary Design Optimization of a Strut-Braced Wing," AIAA Paper 2000-1327, April 2000.
[22] "MSC/NASTRAN 2004—Reference Manual," The Macneal–Schwendler Corp., Santa Ana, CA, 2003.
[23] Morino, L., "A General Theory of Unsteady Compressible Potential Aerodynamics," NASA CR-2464, 1974.
[24] Bindolino, G., Mantegazza, P., and Visintini, L., "A Comparison of Panel Methods for Potential Flow Calculations," *VIII Congresso Nazionale*, Associazione Italiana di Aeronautica e Astronautica, Rome, Italy, Sept. 1985, pp. 59–88.
[25] "OPTIMUS: Theoretical Background," NOESIS Solution, 2006.
[26] Allen, H. J., "Calculation of the Chordwise Load Distribution over Airfoil Sections with Plain, Split, or Serially Hinged Trailing-Edge Flaps," NACA TR-634, 1938.
[27] Niu, M., and Niu, M., *Airframe Structural Design*, Conmilit Press, Hong Kong, 2006.
[28] Macci, S. H., "Semi-Analytical Method for Predicting Wing Structural Mass," Society of Allied Weight Engineers Paper 2282, May 1995.
[29] Murman, E. M., Bailey, F. R., and Johnson, M. L., "TSFOIL-A Computer Code for Two-Dimensional Transonic Calculations, Including Wind-Tunnel Wall Effects and Wave Drag Evaluation," NASA SP-347, March 1975.
[30] Harrison, N., "Boeing 747," *Flight International*, Vol. 94, No. 3118, Dec. 1968, pp. 78–9974.
[31] Jackson, P. (ed.), *Jane's All the World's Aircraft*, IHS Jane's, IHS (Global) Limited, Berkshire, England, UK, 2006.
[32] "Boeing Design Manual—BDM 6001," The Boeing Company, Chicago, IL, 1989.
[33] Frediani, A., Lombardi, G., Chiarelli, M., Longhi, A., D'Alessandro Caprice, M., and Bernardini, G., "Proposal for a New Large Airliner with Non Conventional Configuration," *Proc. of the XIV AIDAA National Congress*, Associazione Italiana di Aeronautica e Astronautica, Rome, Italy, 1997, pp. 333–344.
[34] Frediani, A., Longhi, Chiarelli, M., and Troiani, E., "The Lifting System with Minimum Induced Drag," *Proceedings of the CEAS/DragNet European Drag Reduction Conference*, Springer–Verlag, Berlin, 2001, pp. 312–319.